



# Mass transfer effects on kinetics of the hydrogen oxidation reaction at Nafion film covered Pt/C rotating disk electrodes<sup>☆</sup>

Ren-Bin Lin<sup>a,\*</sup>, Shin-Min Shih<sup>b</sup>, Jian-Lin Liu<sup>a</sup>

<sup>a</sup> Department of Chemical and Materials Engineering, Chinese Culture University, Taipei 11114, Taiwan

<sup>b</sup> Department of Chemical Engineering, National Taiwan University, Taipei 10607, Taiwan

## ARTICLE INFO

### Article history:

Received 26 October 2010

Received in revised form 22 March 2011

Accepted 13 April 2011

Available online 24 May 2011

### Keywords:

Electrocatalysis

Platinum

Hydrogen oxidation

Mass transfer

Fuel cells

## ABSTRACT

The effects of mass transfer on the kinetics of the hydrogen oxidation reaction at the Nafion covered Pt/C electrodes immersed in 0.5 M H<sub>2</sub>SO<sub>4</sub> was investigated using a rotating disk electrode configuration. The hydrodynamic voltammograms were analyzed to determine the kinetic parameters using the modified Koutecky–Levich equation. The permeability of H<sub>2</sub> in the Nafion film was determined to be  $2.0 \times 10^{-5}$  mM cm<sup>2</sup> s<sup>-1</sup>, which is close to that in 0.5 M H<sub>2</sub>SO<sub>4</sub>. Due to the fast intrinsic reaction rate of H<sub>2</sub> oxidation on the Pt catalyst, the diffusion of H<sub>2</sub> in the catalyst layer affected the overall reaction rate to a higher extent when the Pt loading or the overpotential increased. The effect of H<sub>2</sub> diffusion in the catalyst layer on the overall reaction rate was accounted for using the effectiveness factor. The corrected exchange current density for the 20 wt% Pt/C catalyst was determined to be about 0.96 mA cm<sup>-2</sup>, based on the real Pt surface area. The results of this work may contribute to the measurement on the intrinsic electrocatalytic activity of a high surface area catalyst used in proton exchange membrane fuel cells.

© 2011 Elsevier B.V. All rights reserved.

## 1. Introduction

Fuel cell is a clean and efficient alternative fuel technology. Due to its potential economic, energy, and environmental benefits, this technology has been under extensive research and development [1]. Particularly, proton exchange membrane fuel cells (PEMFCs) have recently received more attention due to their high power density at relatively low temperatures and zero emission of air pollutants [2]. The fuel (H<sub>2</sub>) and oxidant gases (O<sub>2</sub> or air) flow past the backside of the anode and cathode, respectively, and react in the zone of the three-phase boundary established at gas/electrolyte/catalyst interface within the electrodes, which are porous structures that have a large interfacial contact area to achieve practical current densities.

Platinum (Pt) is the most widely used electrocatalyst in low-temperature fuel cells [1,3]. Such a Pt catalyst, however, is very expensive. Lowering precious metal loading is desired to reduce the cost and to facilitate the market entry of fuel cells. Accordingly, electrodes were prepared consisting mainly of highly dispersed Pt particles supported on carbon (Pt/C), optimizing their active surface area for the electrocatalytical reaction. This cost require-

ment also led to the ionomer phases (e.g. Nafion) incorporating into the catalyst layer, forming the effective three-phase reaction zone [4–7]. So far, a lot of efforts were made to investigate the influences of the active layer compositions on the fuel cell performance. Most efforts were focused on optimization as a function of Nafion content [8–11]. Nevertheless, Pt catalysts loaded on carbon might not totally serve to electrochemical reactions. Probably half of Pt particles do work as electrocatalysts [12]. This may be related to the nature of the interface between ion-exchange polymer electrolyte and carbon particles with Pt catalysts [13,14]. Since the performance of a fuel cell is affected by the mass transfer, a better understanding of these effects is necessary in order to quantitatively determine the intrinsic activity of a catalyst and to devise such an efficient electrode for the practical operation.

In the present work, the commercial 20 wt% Pt/C catalyst was used and its activity for the H<sub>2</sub> oxidation reaction (HOR) when it was covered with a Nafion film was studied by the rotating disk electrode (RDE) methodology. The kinetic parameters for the H<sub>2</sub> oxidation reaction at the Nafion covered Pt/C electrodes were evaluated with the aim to investigate the mass transfer effects on the reaction kinetics and thus determine the intrinsic activity of the catalyst. Similar study has been carried out by Schmidt et al. [15], but the effect of the Pt loading was not reported and the theoretical description of the rotating thin-film method for the determination of the intrinsic activity of a high surface area catalyst was not discussed in detail.

<sup>☆</sup> The manuscript had been presented at The 13th Asia Pacific Confederation of Chemical Engineering Congress (APCChE 2010), October 5–8, 2010, Taipei, Taiwan.

\* Corresponding author. Tel.: +886 2 28610511; fax: +886 2 28614011.

E-mail address: [lrb@faculty.pccu.edu.tw](mailto:lrb@faculty.pccu.edu.tw) (R.-B. Lin).

## Nomenclature

### Acronyms

CV	cyclic voltammetry
GC	glassy carbon
GPES	general purpose electrochemical system
HOR	hydrogen oxidation reaction
PEMFC	proton exchange membrane fuel cell
RDE	rotating disk electrode
RHE	reversible hydrogen electrode
SCE	saturated calomel electrode
XRD	X-ray diffraction

### Symbols

$a$	surface area per unit catalyst layer volume, $\text{cm}^{-1}$
$B$	Levich constant, $\text{mC cm mol}^{-1}$
$b$	$\exp(nF\eta/RT)$
$C_0$	$\text{H}_2$ solubility in electrolyte, $\text{mol cm}^{-3}$
$C_f$	$\text{H}_2$ solubility in polymer film, $\text{mol cm}^{-3}$
$D$	$\text{H}_2$ diffusivity in electrolyte, $\text{cm}^2 \text{s}^{-1}$
$D_e$	effective diffusivity, $\text{cm}^2 \text{s}^{-1}$
$D_f$	$\text{H}_2$ diffusivity in polymer film, $\text{cm}^2 \text{s}^{-1}$
$E$	potential of an electrode versus a reference, V
$F$	Faraday constant, $96,485 \text{ C mol}^{-1}$
$I$	current of an electrode, mA
$i_d$	diffusion-limited current density, $\text{mA cm}^{-2}$
$i_f$	polymer film diffusion-limited current density, $\text{mA cm}^{-2}$
$i_k$	kinetic current density, $\text{mA cm}^{-2}$
$i_{k,0}$	intrinsic kinetic current density, $\text{mA cm}^{-2}$
$i_m$	measured current density, $\text{mA cm}^{-2}$
$i_0$	exchange current density, $\text{mA cm}^{-2}$
$i_0^*$	corrected exchange current density, $\text{mA cm}^{-2}$
$k$	rate constant for $\text{H}_2$ oxidation reaction, $\text{cm s}^{-1}$
$L$	polymer film thickness, $\mu\text{m}$
$L_c$	catalyst layer thickness, $\mu\text{m}$
$n$	number of electrons involved in the reaction
$Q_{\text{H}}$	hydrogen adsorption/desorption charge, $\text{mC cm}^{-2}$
$Y_0$	Levich intercept, $\text{mA}^{-1} \text{cm}^2$
$R$	gas constant, $8.314 \text{ J mol}^{-1} \text{K}^{-1}$
$r_s$	reaction rate, $\text{mole cm}^{-3} \text{s}^{-1}$
$r_{s,0}$	intrinsic reaction rate, $\text{mole cm}^{-3} \text{s}^{-1}$
$S_g$	specific surface area, $\text{m}^2 \text{g}^{-1}$
$T$	temperature, K
$W_l$	Pt loading, $\mu\text{g cm}^{-2}$
$\alpha$	transfer coefficient
$\eta$	overpotential, mV
$\eta_e$	effectiveness factor
$\delta$	roughness factor of the electrode
$\rho_b$	bulk density of the catalyst layer, $\text{cm}^3 \text{g}^{-1}$
$\nu$	kinematic viscosity, $\text{cm}^2 \text{s}^{-1}$
$\omega$	rotation rate, rpm
$\psi$	Thiele modulus

## 2. Experimental

### 2.1. Materials

The Pt catalyst used was 20 wt% platinum on Vulcan XC-72R carbon black (HiSPEC™ 3000, Johnson Matthey). For brevity, this catalyst was referred to as Pt/C catalyst in this study. The mean particle size of the carbon black,  $4.0 \mu\text{m}$ , was measured by laser diffraction using a Coulter LS-230 analyzer. According to the manufacturer's data, the active Pt surface area was  $110 \text{ m}^2 \text{g}_{\text{Pt}}^{-1}$

determined by gas-phase CO chemisorption. The Pt crystal size was  $2.6 \text{ nm}$  determined by X-ray diffraction (XRD). Glassy carbon (GC) disk electrode (disk area =  $0.1963 \text{ cm}^2$  and shroud area =  $1.131 \text{ cm}^2$ , Pine Instruments) was served as the substrate for the deposition of the catalyst. A Nafion solution containing 5 wt% Nafion dissolved in a mixture of isopropanol and water (1100 equivalent weight, Ion Power) was used to recast the Nafion film. High purity  $\text{H}_2$  gas (99.999%, San-Fu) was used. The electrolyte was  $0.5 \text{ M H}_2\text{SO}_4$  solution prepared from concentrated sulfuric acid (J.T. Baker) and ultrapure water ( $18 \text{ M}\Omega$ , Millipore).

### 2.2. Electrode preparation

An aqueous catalyst suspension of  $2 \text{ mg mL}^{-1}$  was prepared by mixing  $50 \text{ mg}$  of Pt/C catalyst and  $25 \text{ mL}$  of deionized water under ultrasonication for about  $10 \text{ min}$ . Diluter catalyst suspensions, which were necessary to form thinner catalyst layer, were prepared following a similar process with lower catalyst weights. About  $10\text{--}20 \mu\text{L}$  of the catalyst suspension was pipetted onto the disk surface and dried under room temperature. After the catalyst layer was dry, a  $20 \mu\text{L}$  of Nafion solution was put on the top of the catalyst layer. Subsequent annealing in a vacuum oven ( $70^\circ\text{C}$ ) was made for at least  $40 \text{ min}$  to evaporate the residual solvent in the resulting thin-film electrode. This annealing renders the recast film insoluble and with sufficient strength to bind the catalyst particles [16]. The concentration of Nafion solution was varied by diluting the 5 wt% Nafion solution with isopropanol to yield the recast films with thicknesses ranging from  $0.1$  to  $8.0 \mu\text{m}$ . The film thickness was calculated from the mass and the surface area of the recast film, assuming a dry Nafion density of  $1.98 \text{ g cm}^{-3}$  [8,16,17]. It was estimated that about 90% of the shroud surface area was covered, i.e. the geometric area of the Nafion coating was  $\approx 1.0 \text{ cm}^2$ . The film thickness in the range from  $0.5$  to  $3.0 \mu\text{m}$  was further measured using a surface texture profilometer (Dektak 3030, Sloan Technology), and the difference between the measured and calculated values was about 6%. The fabrication procedure of the thin-film rotating disk electrode was similar to that described elsewhere [15,18,19].

### 2.3. Electrochemical measurements

A conventional three-compartment glass cell with a saturated calomel reference electrode (SCE) and a Pt foil counter electrode was used to study the electrochemical behaviors of the thin-film rotating disk electrodes. Electrochemical measurements were conducted at room temperature ( $25 \pm 1^\circ\text{C}$ ) using a potentiostat (Autolab PGSTAT30, Ecochemie) with a computer-controlled general purpose electrochemical system (GPES). Throughout this study, all potentials were referred to the reversible hydrogen electrode (RHE) scale. Before the measurements, the electrode was well hydrated in deaerated  $0.5 \text{ M H}_2\text{SO}_4$  solution, which exhibited a very similar pH value to that of the Nafion film. Characteristic cyclic voltammograms (CVs) were obtained after scanning the potential of the electrode between  $0$  and  $1 \text{ V}$  versus RHE for hundreds of cycles. This long run-in period was necessary to obtain stable and reproducible data. Experiments for  $\text{H}_2$  oxidation on the Nafion film covered Pt/C rotating disk electrodes were performed in  $\text{H}_2$ -saturated  $0.5 \text{ M H}_2\text{SO}_4$  electrolyte at several rotation rates in the range from  $400$  to  $3600 \text{ rpm}$ .  $\text{H}_2$  was passed through the solution for  $40 \text{ min}$  before the experiment started and above the solution during the experiment. The potential of the electrode was changed between  $0$  and  $0.15 \text{ V}$  versus RHE at a scan rate of  $5 \text{ mV s}^{-1}$ .

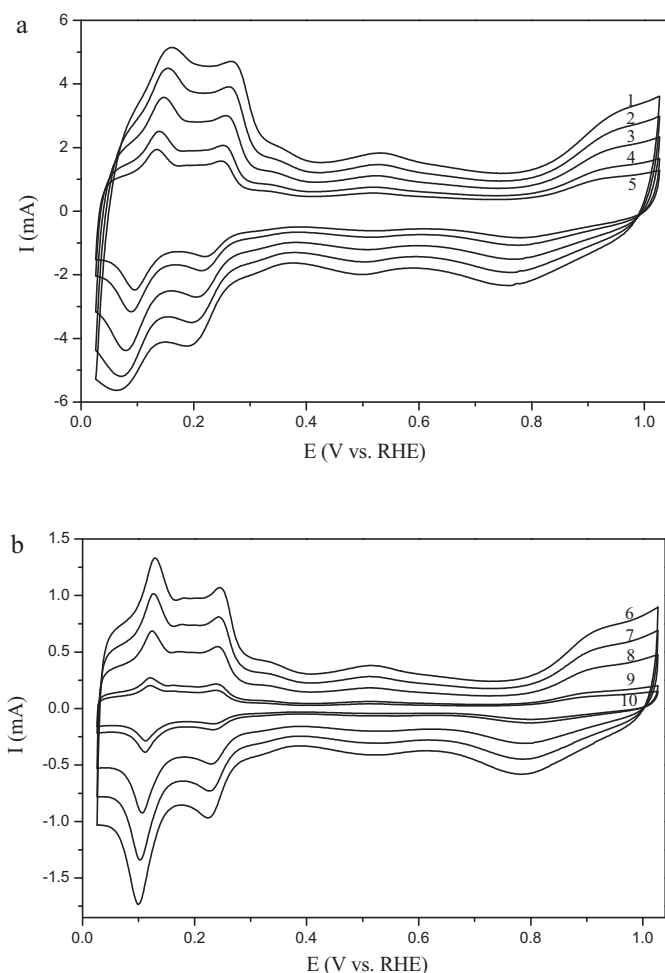


**Fig. 1.** Cyclic voltammograms on the Nafion covered Pt/C electrode (Pt loading:  $40.8 \mu\text{g cm}^{-2}$ ; Nafion film thickness:  $0.2 \mu\text{m}$ ). Various scan rates ( $\text{mVs}^{-1}$ ): (a) (1) 500, (2) 400, (3) 300, (4) 200, (5) 150; (b) (6) 100, (7) 75, (8) 50, (9) 20, (10) 15.

### 3. Results and discussion

#### 3.1. Cyclic voltammetry

The typical cyclic voltammograms for the Nafion film covered Pt/C electrodes are represented in Fig. 1 for an electrode having a Pt loading of  $40.8 \mu\text{g cm}^{-2}$  and a Nafion film thickness of  $0.2 \mu\text{m}$  at various scan rates ( $15\text{--}500 \text{ mVs}^{-1}$ ). One can see that the general shapes of all the curves obtained at different scan rates are very similar and that the characteristic peaks become higher and broader, and shift to the right (anodic scan) or to the left (cathodic scan) as the scan rate increases. Two well-resolved H-adsorption or desorption peaks are observed. For the curve obtained at  $20 \text{ mVs}^{-1}$ , which is similar to the CV reported by Schmidt et al. [15] for their Nafion coated on a layer of 20 wt% Pt/C catalyst, one H-desorption peak is located around 120 mV and the other is located around 238 mV. In the literature [12,20], these two peaks are referred to the desorption of weakly and strongly adsorbed hydrogen, respectively. The weakly adsorbed hydrogen is on Pt (110) or Pt (111) surface, and the strongly adsorbed hydrogen is on Pt (100) surface [15,20]. It has to be noted that the potential of the electrode was scanned below 1.0 V versus RHE in order to avoid the significant surface oxidation of carbon black at higher potentials [21].

The hydrogen adsorption/desorption charge,  $Q_H$ , was calculated, which was taken as one half of the net charge evaluated by first integrating the currents for both cathodic and anodic scans with time

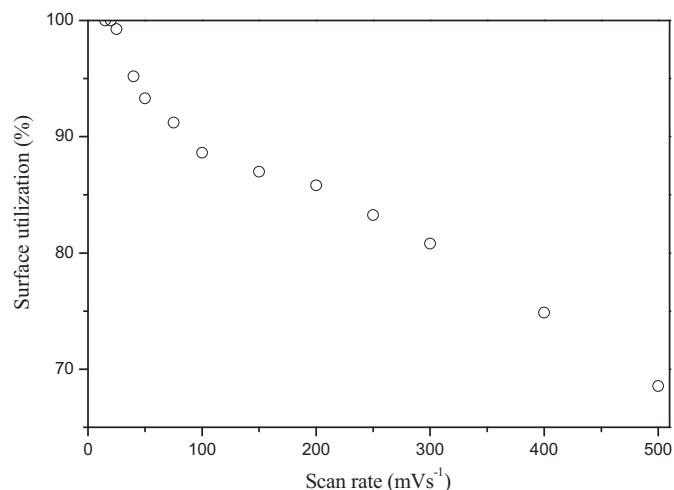


**Fig. 2.** The dependence of catalyst surface utilization on the scan rate for the electrode (Pt loading:  $40.8 \mu\text{g cm}^{-2}$ ; Nafion film thickness:  $0.2 \mu\text{m}$ ).

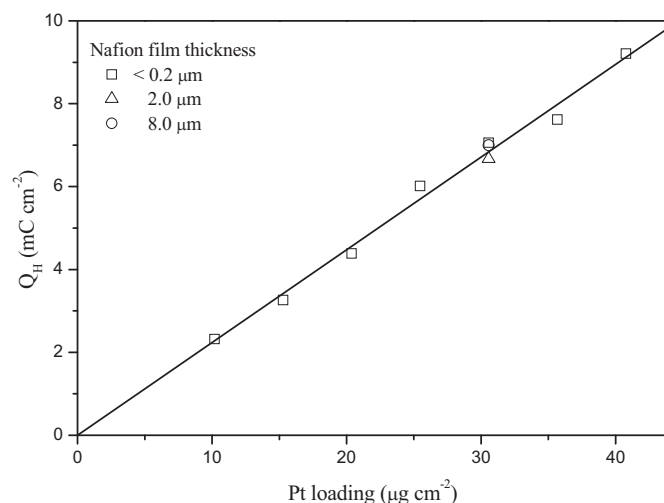


**Fig. 3.** The charge in the hydrogen adsorption/desorption region versus Pt loading. Scan rate:  $20 \text{ mVs}^{-1}$ .

in the potential range between 0.05 and 0.4 V and then subtracting the charge for the double layer [17–19].

The electrochemical surface area was determined from the  $Q_H$  value using a surface charge for polycrystalline Pt ( $0.210 \text{ mC cm}^{-2}$ ) [17]. The catalyst surface utilization was then calculated from the ratio of the electrochemical surface area to the actual catalyst surface area ( $110 \text{ m}^2 \text{ g}_{\text{Pt}}^{-1}$ ). The catalyst surface utilization determined at different scan rates are plotted in Fig. 2. As can be seen from the figure, at scan rates  $\leq 20 \text{ mVs}^{-1}$  the electrode has 100% catalyst surface utilization, and above  $20 \text{ mVs}^{-1}$  the surface utilization decreases as the applied scan rate increases. The decrease in catalyst surface utilization measured at high scan rates was due to the incomplete H-adsorption process caused by the ohmic potential drop in the solution [22], which resulted in the measured electrode potential being lower than the real one during the cathodic scan. The ohmic potential drop became more appreciable when the roughness factor of an electrode or the scan rate increased, due to the increase in the current. The catalyst surface area of an electrode can be accurately estimated through CV, if a scan rate that does not cause an appreciable ohmic potential drop is used; the appropriate scan rate became lower as the roughness factor of the electrode increases.

As shown in Fig. 3, for the electrodes with a Nafion film thickness lower than  $0.2 \mu\text{m}$  and Pt loadings ranging from  $10.2$  to  $40.8 \mu\text{g cm}^{-2}$ , the  $Q_H$  evaluated at  $20 \text{ mV s}^{-1}$  was a linear function (a correlation coefficient of  $0.995$ ) of the Pt loading. The value of the slope ( $0.224 \text{ mC } \mu\text{g}^{-1}$ ) was almost identical with that ( $0.231 \text{ mC } \mu\text{g}^{-1}$ ) calculated from the Pt weight, active Pt surface area ( $110 \text{ m}^2 \text{ g}^{-1}$ ), and the surface charge for polycrystalline Pt [17]. This result demonstrates that the electrochemical surface area of an electrode measured at  $20 \text{ mV s}^{-1}$  is essentially the same as the real total surface area of Pt on the electrode.

Additionally, it was found that at the same Pt/C loading, the  $Q_H$  values measured for electrodes with Nafion film thicknesses ranged from  $0.1$  to  $8.0 \mu\text{m}$  were essentially identical (within the experimental errors), as shown in Fig. 3 for the Pt loading at  $30.6 \mu\text{g cm}^{-2}$ . This result seems to reveal that no matter how thick the Nafion film was, only little penetration of the Nafion binder into the catalyst layer could occur, and the direct contact between the Nafion film and the catalyst layer was limited to the skin surface of the catalyst layer. Thus, the possible site-blocking effect of Nafion for hydrogen electrochemical processes would be very small. Besides, the result also indicates that the diffusional resistance for  $\text{H}^+$  ions in the Nafion film was negligible for the H-adsorption/desorption processes even the film was as thick as  $8.0 \mu\text{m}$ .

In order to investigate the reproducibility of electrode preparation, the  $Q_H$  measurements were performed for electrodes prepared independently with a Pt loading of  $40.8 \mu\text{g cm}^{-2}$  (Nafion film thickness of  $\approx 0.2 \mu\text{m}$ ). The variation in  $Q_H$  ( $9.22 \pm 0.31 \text{ mC cm}^{-2}$ ) gave a standard deviation of  $\pm 3.4\%$ . This result also indicates that the  $Q_H$  measurements were sufficiently accurate.

### 3.2. Kinetics of $\text{H}_2$ oxidation reaction

Experiments for  $\text{H}_2$  oxidation were conducted on the Nafion film covered Pt/C electrodes for which the Pt loading varied from  $10.2$  to  $20.4 \mu\text{g cm}^{-2}$  and the Nafion film thickness varied from  $0.1$  to  $8.0 \mu\text{m}$ . The hydrodynamic voltammograms for the electrodes having a Pt loading of  $10.2 \mu\text{g cm}^{-2}$  and Nafion film thicknesses of  $0.1$  and  $8.0 \mu\text{m}$  are represented in Fig. 4. One can see that the current density increases with increasing rotation rate and that the current density is larger when the Nafion film is thinner at the same rotation rate. The current density initially increases with increasing overpotential and reaches a limiting value when the overpotential is about  $70 \text{ mV}$  versus RHE.

For a RDE without a Nafion film, if  $\text{H}_2$  oxidation reaction is totally irreversible, the measured current density,  $i_m$ , for the electrode reaction is given by

$$\frac{1}{i_m} = \frac{1}{i_k} + \frac{1}{i_d} \quad (1)$$

where  $i_k$  represents the kinetic current density in the absence of mass transfer effect in the aqueous electrolyte. The boundary-layer diffusion-limited current density,  $i_d$ , can be expressed by the Levich equation [22]:

$$i_d = 0.62nFD^{2/3}\nu^{-1/6}C_0\omega^{1/2} = BC_0\omega^{1/2} \quad (2)$$

where  $n$  is the number of electrons involved in the electrode reaction,  $F$  is the Faraday constant,  $D$  is the reactant diffusivity in the electrolyte,  $\nu$  is the electrolyte kinematic viscosity,  $C_0$  is the reactant solubility in the electrolyte, and  $\omega$  is the rotation rate.

For a RDE with a Nafion film, besides the diffusion in the aqueous electrolyte, the diffusion in the Nafion film must be taken into account. The measured current density for this case [8,15,18] is given by

$$\frac{1}{i_m} = \frac{1}{i_k} + \frac{1}{i_f} + \frac{1}{i_d} = \frac{1}{i_k} + \frac{1}{i_f} + \frac{1}{BC_0\omega^{1/2}} \quad (3)$$

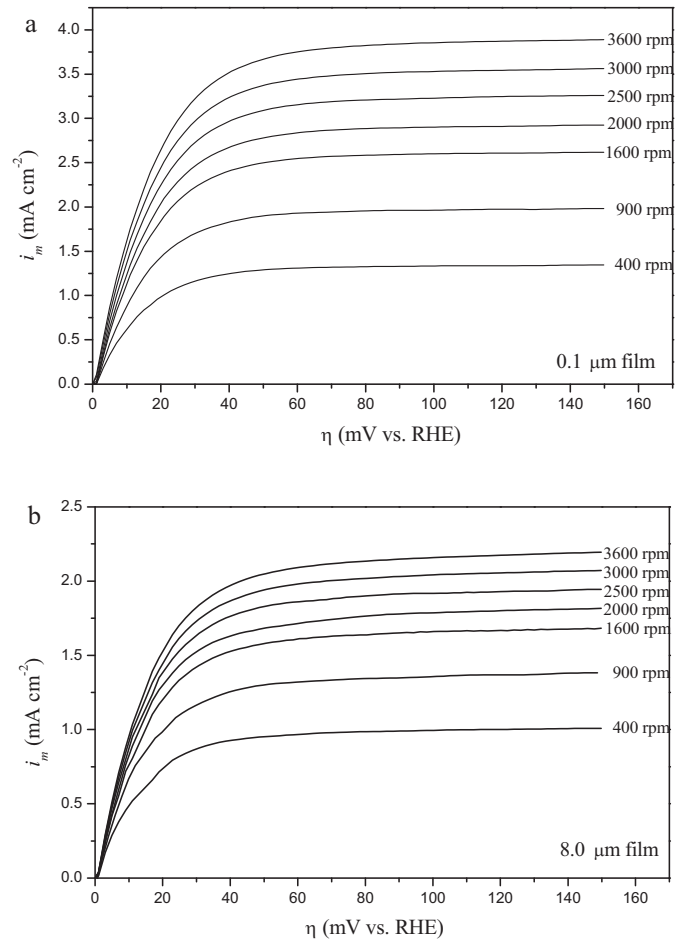


Fig. 4. Hydrodynamic voltammograms for  $\text{H}_2$  oxidation on the Nafion film covered Pt/C electrodes (Pt loading:  $10.2 \mu\text{g cm}^{-2}$ ) with the film thicknesses of (a)  $0.1 \mu\text{m}$  and (b)  $8.0 \mu\text{m}$  in  $\text{H}_2$ -saturated  $0.5 \text{ M H}_2\text{SO}_4$  electrolyte. Scan rate:  $5 \text{ mV s}^{-1}$ .

where  $i_f$  represents the Nafion film diffusion-limited current density, that is the current density measured when the reaction rate is controlled solely by the reactant diffusion in the Nafion film. In this case,  $i_f$  and  $i_k$  can be defined as

$$i_f = nFC_fD_fL^{-1} \quad (4)$$

$$i_k = nF\delta k_f C_0 = i_0 \exp\left(\frac{(1-\alpha)nF\eta}{RT}\right) \quad (5)$$

where  $C_f$  and  $D_f$  stand for the solubility and the diffusivity of the reactant in the film, respectively, and  $C_f D_f$  is its permeability,  $L$  is the film thickness,  $\delta$  is the roughness factor of the electrode surface,  $k_f$  is the rate constant for  $\text{H}_2$  oxidation reaction,  $i_0$  is the exchange current density,  $\alpha$  is the transfer coefficient, and  $\eta$  is the overpotential. Eq. (3) shows that  $1/i_m$  is a linear function of  $\omega^{-1/2}$  with a slope equal to  $1/BC_0$  and an intercept,  $Y_0$ , corresponding to

$$Y_0 = \frac{1}{i_k} + \frac{1}{nFC_fD_fL^{-1}} \quad (6)$$

According to Eq. (6),  $Y_0$  approaches to  $1/i_k$  when  $L$  is sufficiently small.

If  $\text{H}_2$  oxidation reaction is quasi-reversible and the electrolyte is strongly acidic, the current-potential equation [9,22] for a RDE with a Nafion film is

$$\frac{1}{i_m} = \frac{b}{b-1} \left( \frac{1}{i_k} + \frac{1}{nFC_fD_fL^{-1}} + \frac{1}{BC_0\omega^{1/2}} \right) \quad (7)$$

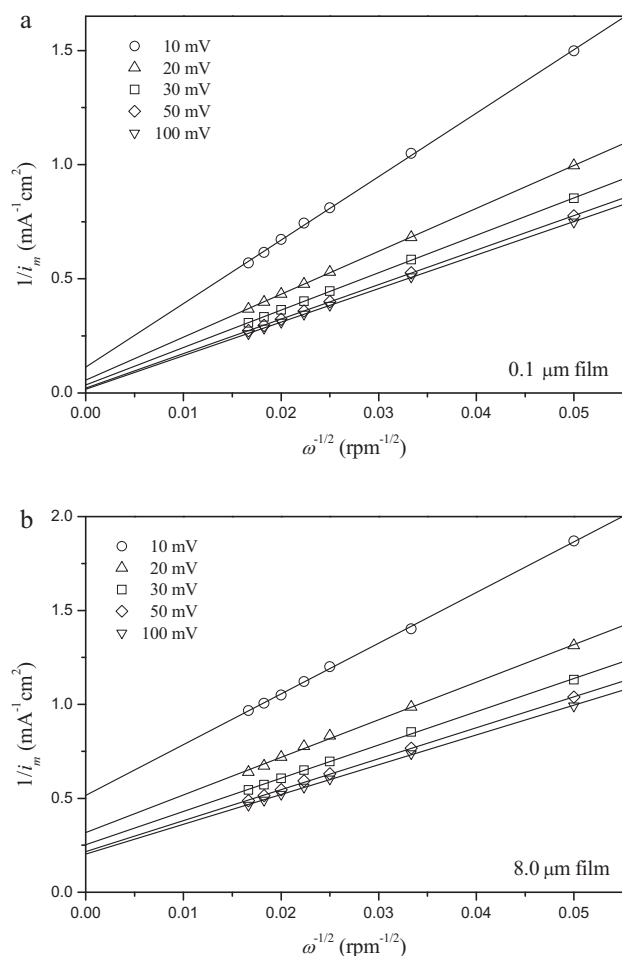


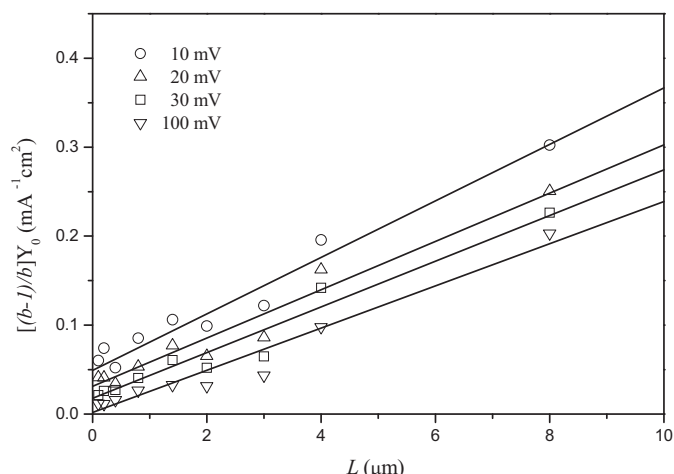
**Fig. 5.** Modified Koutecky–Levich plots for  $\text{H}_2$  oxidation at various overpotentials on the electrodes (Pt loading:  $10.2 \mu\text{g cm}^{-2}$ ) with the Nafion film thicknesses of (a)  $0.1 \mu\text{m}$  and (b)  $8.0 \mu\text{m}$ , respectively.

where  $b = \exp(nF\eta/RT)$ . Eq. (7), the modified Koutecky–Levich equation [9], is still a linear function of  $\omega^{-1/2}$ , but the slope and intercept are affected by the value of overpotential. In this case, the intercept  $Y_0$  is

$$Y_0 = \left( \frac{b}{b-1} \right) \left( \frac{1}{i_k} + \frac{1}{nFC_f D_f L^{-1}} \right) \quad (8)$$

The kinetic parameters for the hydrogen oxidation reaction,  $BC_0$ ,  $C_f D_f$ ,  $i_k$ , and  $i_0$ , can be estimated by analyzing the  $i_m$  data obtained at different overpotentials, rotation rates, and film thicknesses using the above equations.

Fig. 5 shows the modified Koutecky–Levich plots [9,22] of the data obtained at various overpotentials for the Nafion film thicknesses of  $0.1$  and  $8.0 \mu\text{m}$ . As demonstrated by the plots, the data agree with the prediction of Eq. (7) rather than that of Eq. (3); the slope of the linear fitting line changes with the overpotential and agrees with the expectation from the corresponding  $b/(b-1)$  value for the respective overpotential. Nevertheless, Eq. (3) is valid at sufficiently large overpotentials ( $\geq 100\text{mV}$ ), where  $b/(b-1) \approx 1$ . The average value of  $BC_0$  determined at the overpotential of  $100\text{mV}$  for all the electrodes,  $6.49 \times 10^{-2} \text{ mA cm}^{-2} \text{ rpm}^{-1/2}$  ( $\pm 4.1\%$ ), is in excellent agreement with the value at  $298\text{K}$ ,  $6.54 \times 10^{-2} \text{ mA cm}^{-2} \text{ rpm}^{-1/2}$ , calculated from Eq. (2) by Gasteiger et al. [23] using  $D = 3.7 \times 10^{-5} \text{ cm}^2 \text{ s}^{-1}$ ,  $\nu = 1.07 \times 10^{-2} \text{ cm}^2 \text{ s}^{-1}$ , and  $C_0 = 7.14 \times 10^{-4} \text{ M}$ .



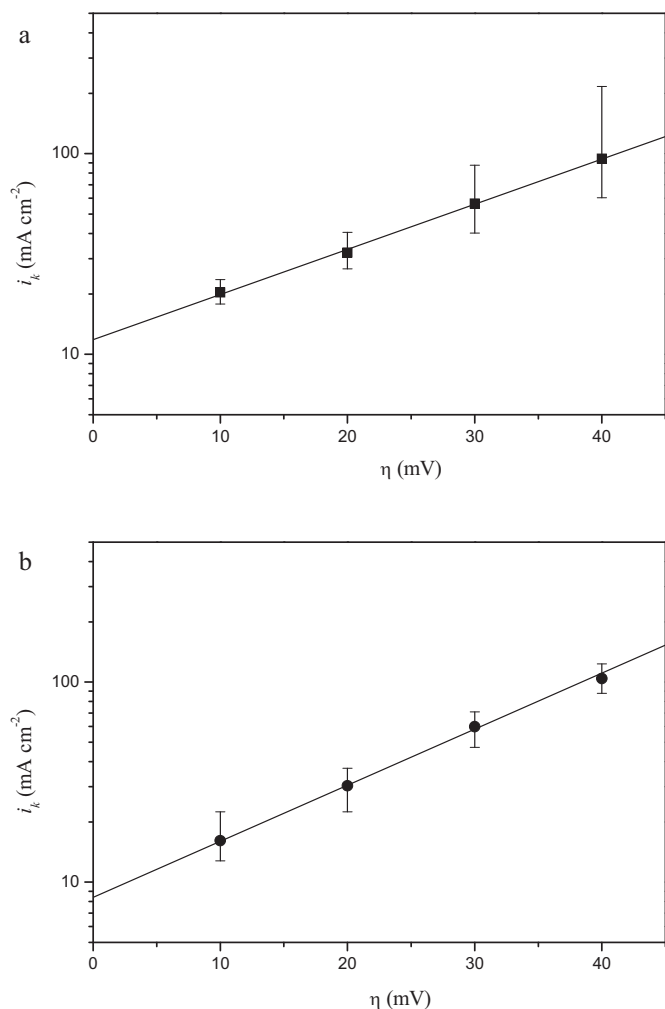
**Fig. 6.**  $[(b-1)/b]Y_0$  versus  $L$  plots for  $\text{H}_2$  oxidation on the Nafion covered Pt/C electrodes (Pt loading:  $10.2 \mu\text{g cm}^{-2}$ ) at several overpotentials.

Fig. 6 shows the plots of  $[(b-1)/b]Y_0$  versus Nafion film thickness ( $L$ ) at several overpotentials. As seen in the figure, although the data are somewhat scattering, they show the linear relationship according to Eq. (8), and the slopes of the fitting lines are essentially equal. This result demonstrates that the  $C_f D_f$  value is independent of both the Nafion film thickness and the overpotential. From the linear fitting of the data shown in Fig. 6 using Eq. (8), the average value of  $C_f D_f$  was determined to be  $2.0 \times 10^{-5} \text{ mM cm}^2 \text{ s}^{-1}$  ( $\pm 10\%$ ). This value is higher than most values reported in the literature [8,9,24]. For instance, a  $C_f D_f$  value of  $1.2 \times 10^{-5} \text{ mM cm}^2 \text{ s}^{-1}$  for recast Nafion films immersed in  $0.1 \text{ M HClO}_4$  was reported by Maruyama et al. [9], and  $9.0 \times 10^{-6} \text{ mM cm}^2 \text{ s}^{-1}$  for those immersed in  $0.5 \text{ M H}_2\text{SO}_4$  was reported by Mello and Ticianelli [24]. The discrepancy in the  $C_f D_f$  value for recast Nafion films can be explained partly by the errors in the experimental measurements, especially in the estimation of the film thickness, and partly by the difference in the structural properties of the Nafion film, such as the pore size and the distribution of the hydrophilic and hydrophobic phases, which are known to affect the  $C_f D_f$  values significantly [9]. It should be noted that the recast Nafion films investigated in this study are much thinner than those used in the previous investigations [9,24].

The kinetic current densities at different overpotentials can be obtained from the intercepts of the fitting lines in Fig. 7 (method a). As shown in Fig. 7a, the semi-logarithm plot of  $i_k$  versus  $\eta$  is linear as expected by Eq. (5). From the intercept of the fitting line, the exchange current density,  $i_0$ , was determined to be  $12.3 \text{ mA cm}^{-2}$  ( $\pm 26\%$ ) for a Pt loading of  $10.2 \mu\text{g cm}^{-2}$ . From the slope of the fitting line, the transfer coefficient,  $\alpha$ , was determined to be  $0.36$ .

Alternatively, the kinetic current density can be calculated from the values of  $Y_0$  and  $L/(nC_f D_f)$  using Eq. (8) (method b). The value of  $L/(nC_f D_f)$  for each Nafion film thickness was taken as the  $Y_0$  value at the overpotential of  $100\text{mV}$ , where  $i_k$  is sufficiently large to satisfy the criteria of both  $1/i_k \approx 0$  and  $b/(b-1) \approx 1$ . The  $i_k$  values at lower overpotentials were then calculated for various Nafion film thicknesses. The average  $i_k$  values thus obtained at different overpotentials are shown in Fig. 7b. One can see that the uncertainty in  $i_k$  for method b is smaller than that for method a in general, as indicated by the upper and lower bars for the range of  $i_k$  values. From this set of data, the  $\alpha$  value determined,  $0.17$ , is smaller than that for method a, but the value of  $i_0$  determined,  $8.4 \text{ mA cm}^{-2}$  ( $\pm 19\%$ ), is close to that for method a. This agreement demonstrates that the two methods are adequate for the evaluation of the exchange current density. However, method b gave results with less uncertainties than method a. The  $i_0$  values determined above are based on the geometric area of an electrode. For the electrode with a Pt





**Fig. 7.** The dependence of kinetic current density on the overpotential for H<sub>2</sub> oxidation on the electrodes (Pt loading: 10.2 μg cm<sup>-2</sup>). (a) Method a and (b) method b.

**Table 1**

Effect of Pt/C loading on the  $i_0$  and  $\alpha$  values determined for the hydrogen oxidation reaction on Nafion film covered Pt/C electrodes in 0.5 M H<sub>2</sub>SO<sub>4</sub>; Nafion film thickness: 0.1 μm.

Pt loading (μg cm <sup>-2</sup> )	$i_0$ (mA cm <sup>-2</sup> )		$\alpha$
	Based on geometric area	Based on real surface area	
10.2	8.4 ± 1.6	0.75 ± 0.14	0.17
15.3	10.4 ± 2.0	0.62 ± 0.12	0.15
20.4	10.1 ± 1.9	0.45 ± 0.08	0.21

loading of 10.2 μg cm<sup>-2</sup> ( $\delta \approx 11.2$ ), the exchange current density based on the real Pt surface area of the electrode was determined to be 0.75 ± 0.14 mA cm<sup>-2</sup>.

The effect of Pt loading on the kinetics of H<sub>2</sub> oxidation reaction was also investigated, and the  $i_0$  and  $\alpha$  values determined using method b are listed in Table 1. The  $\alpha$  values measured for all the Pt/C loadings were essentially identical, indicating that in general the  $\alpha$  value is potential-independent under the overpotential range ≤ 40 mV. One can see that the  $i_0$  values based on the real surface area become smaller as the Pt loading increases from 10.2 to 20.4 μg cm<sup>-2</sup>, but those based on the geometric area are about the same. This result indicates that only a portion of the total surface area of the Pt particles loaded was utilized in the reaction for those

thicker catalyst layers. This is attributed to the H<sub>2</sub> mass-transfer resistance in the catalyst layer. The effect of mass transfer in the catalyst layer on the  $i_k$  and  $i_0$  values will be analyzed in the following section.

### 3.3. Mass transfer effects in catalyst layer

The diffusional effect of H<sub>2</sub> on the overall reaction rate of the catalyst layer can be represented by the effectiveness factor [25],  $\eta_e$ , which is the ratio of the rate ( $r_s$ ) affected by the diffusion of H<sub>2</sub> in the catalyst layer to that ( $r_{s,0}$ ) unaffected.

$$\eta_e = \frac{r_s}{r_{s,0}} = \frac{\tanh \psi}{\psi} \quad (9)$$

The value of  $\psi$  is required to calculate  $\eta_e$ . However, because  $k$  is the unknown to be determined, Eq. (10) cannot be used to obtain  $\psi$ . Instead, Eq. (11) can be used to estimate  $\psi$  from  $i_k$ ,  $C_0$ ,  $D_e$ , and  $L_c$  are known.

$$\psi = L_c \sqrt{\frac{ka}{D_e}} \quad (10)$$

$$i_k = \frac{nFD_eC_0}{L_c} \psi \tanh \psi \quad (11)$$

Alternatively, if  $i_k$  values for two or more catalyst layer thicknesses are available,  $\psi$  for each catalyst layer can be determined without knowing  $C_0$  and  $D_e$ . From Eqs. (10) and (11), we have the following equations for two thicknesses 1 and 2 under the same  $\eta$  and  $C_0$ :

$$\frac{\tanh((L_{c1})/(L_{c2})\psi_2)}{\tanh \psi_2} = \frac{i_{k1}}{i_{k2}} \quad (12)$$

$$\psi_1 = \frac{L_{c1}}{L_{c2}} \psi_2 \quad (13)$$

Therefore, except  $i_k$ 's, only the ratio of two layer thicknesses is required to obtain  $\psi$ 's. The layer thickness is related to the Pt loading ( $W_l$ ) by

$$L_c = \frac{W_l}{\rho_b} \quad (14)$$

where  $\rho_b$  is the bulk density of the catalyst layer.

Thus, the ratio of catalyst layer thicknesses equals the ratio of Pt loadings, if the catalyst layers have the same bulk density.

This method, however, is not valid when  $\psi$  is large ( $\psi > 3$ ). For this case,  $i_k$  is independent of layer thickness as shown by Eq. (15) and the ratio of two current densities is unity [26,27].

$$i_k = nFC_0(D_e ka)^{1/2} \quad (15)$$

From Eq. (16), the ratio of current densities for two layer thicknesses under the same  $\eta$  and  $C_0$  is written as Eq. (17)

$$i_k = \eta_e \delta i_0^* b^{1-\alpha} \quad (16)$$

$$\frac{i_{k1}}{i_{k2}} = \frac{\eta_{e1} \delta_1}{\eta_{e2} \delta_2} \quad (17)$$

The roughness factor  $\delta$  can be calculated from

$$\delta = S_g W_l \quad (18)$$

where  $S_g$  is the specific surface area of Pt. Thus, the ratio of  $\delta$ 's is the same as the ratio of Pt loadings, if the catalyst layers have the same  $S_g$ . Hence, if one  $\eta_e$  value is known, the other one can be estimated using Eq. (17), and the corresponding  $\psi$  value then can be determined from Eq. (9).

Once the  $\eta_e$  and  $\psi$  values are known,  $i_{k,0}$  and  $D_e$  can be determined from  $i_k$  value using Eqs. (19) and (11), respectively.

$$i_k = \eta_e i_{k,0} \quad (19)$$

**Table 2**Values of  $i_k$  ( $\text{mA cm}^{-2}$ ),  $i_{k,0}$  ( $\text{mA cm}^{-2}$ ), and  $\eta_e$  for the Nafion film covered Pt/C electrodes. Nafion film thickness: 0.1  $\mu\text{m}$ .

Overpotential (mV)	Pt loading ( $\mu\text{g cm}^{-2}$ )								
	10.2			15.3			30.6		
	$i_k$	$\eta_e$	$i_{k,0}$	$i_k$	$\eta_e$	$i_{k,0}$	$i_k$	$\eta_e$	$i_{k,0}$
5	11.1	0.82	13.6	14.2	0.64	22.2	15.4	0.34	45.4
10	16.0	0.79	20.3	19.6	0.61	32.3	21.2	0.32	66.6
15	21.6	0.61	35.5	18.6	0.36 <sup>a</sup>	51.6 <sup>a</sup>	23.7	0.22	109.1
20	34.3	0.71	48.6	38.8	0.46	83.3	42.8	0.32	134.4
25	48.6	0.63	77.8	50.9	0.49	103.5	64.0	0.39	162.8
30	69.5	0.73	95.8	78.4	0.59	132.0	92.4	0.38	245.3

<sup>a</sup> Estimated using Eq. (17).

In the following calculations, Eqs. (12) and (13) were used to estimate  $\psi$ 's. If these equations failed, then Eq. (17) was used.

For the Nafion film covered Pt/C electrodes, the measured  $i_k$  values together with the  $\eta_e$  and  $i_{k,0}$  values estimated from Eqs. (9) and (19) are summarized in Table 2. As seen in Table 2, the values of  $\eta_e$  are in the range of 0.22–0.82. The  $\eta_e$  value decreases markedly with increasing Pt loading for a given overpotential, but it is insensitive to the overpotential in general. The  $i_{k,0}$  value in general is proportional to the Pt loading as expected by Eq. (20), but the proportionality is better at low overpotentials ( $\leq 20$  mV) than at high overpotentials. The deviations from what expected can be explained by the greater uncertainties in the experimental  $i_k$  values obtained at high overpotentials (see Fig. 7). As shown in Fig. 8, the semi-logarithm plots of the  $i_{k,0}$  value versus the overpotential are linear as predicted by Eq. (20).

$$i_{k,0} = \delta i_0^* b^{1-\alpha} \quad (20)$$

From the slope and intercept of the fitting line for each Pt loading, the corrected  $\alpha$  and exchange current density ( $i_0^*$ ) were determined. The values of  $i_0^*$  and  $\alpha$  for each Pt loading are listed in Table 3. The average value of  $i_0^*$  is  $0.96 \pm 0.10 \text{ mA cm}^{-2}$ , based on the real Pt surface area. The corrected exchange current density is undoubtedly higher than the apparent one ( $0.75 \pm 0.14 \text{ mA cm}^{-2}$ ) estimated in the preceding section.

The above results indicate that the hydrogen oxidation reaction in the catalyst layer was affected by the  $\text{H}_2$  diffusion. The assumptions and equations employed are adequate to account for the  $\text{H}_2$  mass-transfer resistance in the catalyst layer and to determine the intrinsic kinetic parameters.

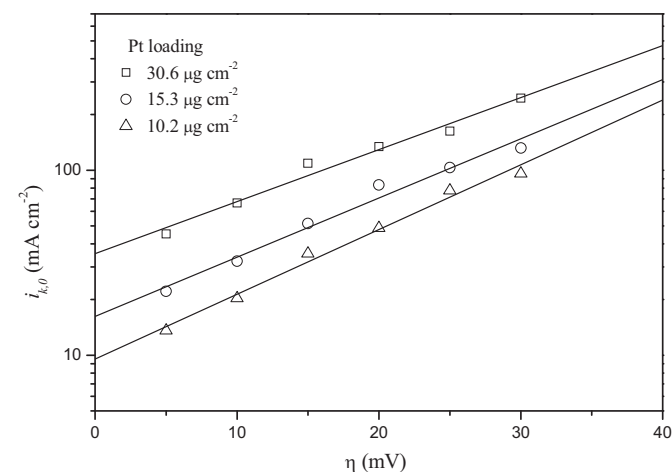


**Fig. 8.** The dependence of intrinsic kinetic current density on the overpotential for  $\text{H}_2$  oxidation on the Nafion film covered Pt/C electrodes with several Pt loadings (Nafion film thickness: 0.1  $\mu\text{m}$ ).

**Table 3**Values of  $i_0^*$  and  $\alpha$  for the Nafion film covered Pt/C electrodes. Nafion film thickness: 0.1  $\mu\text{m}$ .

Pt loading ( $\mu\text{g cm}^{-2}$ )	$i_0^*$ ( $\text{mA cm}^{-2}$ )	$\alpha$
10.2	0.85	0
15.3	0.97	0.05
30.6	1.05	0.17
Average	0.96	

### 3.4. Discussion on exchange current density

The  $i_0^*$  value,  $0.96 \text{ mA cm}^{-2}$ , obtained for the Nafion film covered Pt/C electrodes in 0.5 M  $\text{H}_2\text{SO}_4$  at 298 K is evidently larger than that,  $0.49 \text{ mA cm}^{-2}$ , obtained for the Nafion film covered Pt-black electrodes [28]. This result indicates that the intrinsic activity of the Pt/C catalyst is higher than that of the Pt-black catalyst. The  $i_0$  value,  $0.96 \text{ mA cm}^{-2}$ , obtained for Nafion film covered Pt/C electrodes in 0.5 M  $\text{H}_2\text{SO}_4$  at 298 K is evidently larger than that,  $0.25 \text{ mA cm}^{-2}$ , reported by Jiang and Kuecernak [29] for their porous Pt micro-electrodes in 0.5 M  $\text{H}_2\text{SO}_4$  at 293 K. However, our  $i_0$  value is smaller than that,  $1.62 \text{ mA cm}^{-2}$ , obtained by Maruyama et al. [9] for a Nafion coated smooth Pt electrode in 0.1 M  $\text{HClO}_4$ . Markovic et al. [30] found that the exchange current density for the  $\text{H}_2$  oxidation on Pt is unique with respect to the crystal surfaces. From their results obtained in 0.05 M  $\text{H}_2\text{SO}_4$ , the  $i_0$  values on Pt (1 1 0), Pt (1 0 0), and Pt (1 1 1) surfaces at 298 K were estimated to be 0.92, 0.55, and  $0.40 \text{ mA cm}^{-2}$ , respectively. It is known that the dominant crystal surfaces for small particles change with the Pt particle diameters [13]. Also, electrolytes with different pH values may be used, and the  $\text{H}_2$  solubility in an electrolyte would vary with the type of electrolyte and the  $\text{H}_2$  partial pressure. Thus, the differences between the exchange current densities measured could be caused by the variations in the relative abundance of Pt crystal surfaces and the differences in experimental conditions.

Another possible reason is that the  $i_k$  values used to obtain  $i_0$  contain great uncertainties [19]. Because the  $i_k$  values are estimated from the  $i_m$  values according to Eq. (7), the uncertainties in  $i_k$  values are proportional to the  $i_k/i_m$  ratios. Since the  $i_k$  values estimated are several ten-fold greater than the  $i_m$  values (see Figs. 4 and 7), the  $i_k$  values are inherently subjected to great uncertainties. Besides, the deviation from the ideal case of uniform layer thickness and flat surface is unavoidable in practice and different extent of deviation may result, depending on the operation of the deposition process. Thus, the carefulness in the deposition process will reduce the uncertainty and improve the reproducibility of the  $i_0$  values determined.

## 4. Conclusions

The electrochemical behaviors of the Nafion film covered Pt/C electrodes and their electrocatalytic activities toward  $\text{H}_2$  oxidation

were investigated by cyclic voltammetry and rotated disk voltammetry. At scan rates  $\leq 20 \text{ mV s}^{-1}$ , the thin-film electrode has 100% catalyst surface utilization. However, when the scan rate is sufficiently rapid, a decrease in catalyst utilization with increasing scan rate is consequently observed. The diffusion resistance of  $\text{H}^+$  ions due to the Nafion coating is negligible due to the complete wetting. However, the current density for  $\text{H}_2$  oxidation was reduced by the presence of Nafion coating. The hydrodynamic voltammograms were analyzed to determine the kinetic parameters using the modified Koutecky–Levich equation. The permeability of  $\text{H}_2$  in the Nafion film was determined to be  $2.0 \times 10^{-5} \text{ mM cm}^2 \text{ s}^{-1}$ , which is close to that in  $0.5 \text{ M H}_2\text{SO}_4$ . Due to the fast intrinsic reaction rate of  $\text{H}_2$  oxidation on the catalyst, the diffusion of  $\text{H}_2$  in the catalyst layer affected the overall reaction rate to a higher extent when the Pt loading or overpotential increased. The effect of  $\text{H}_2$  diffusion in the catalyst layer on the overall reaction rate was accounted for using the effectiveness factor. The values of effectiveness factor were estimated from the apparent reaction rates of the catalyst layer at different Pt loadings, using the general effectiveness factor assumptions. The corrected exchange current density for the 20 wt% Pt/C catalyst was determined to be about  $0.96 \text{ mA cm}^{-2}$ , based on the real Pt surface area.

This study is helpful to get more thorough understanding of the kinetics of the  $\text{H}_2$  oxidation reaction and the mass transfer of  $\text{H}_2$  in the catalyst layer and the Nafion film.

### Acknowledgement

The authors would like to express sincere appreciation to the National Science Council (Taiwan) for the financial support.

### References

- [1] K. Kordesch, G. Simader, *Fuel Cells and their Application*, VCH, New York, 1996.
- [2] T.R. Ralph, *Platinum Metals Rev.* 41 (1997) 102.
- [3] V. Mehta, J.S. Cooper, *J. Power Sources* 114 (2003) 32.
- [4] M.S. Wilson, S. Gottesfeld, *J. Electrochem. Soc.* 139 (1992) L28.
- [5] M.S. Wilson, S. Gottesfeld, *J. Appl. Electrochem.* 22 (1992) 1.
- [6] M. Uchida, Y. Aoyama, N. Eda, A. Ohta, *J. Electrochem. Soc.* 142 (1995) 463.
- [7] M.S. Wilson, J.A. Valerio, S. Gottesfeld, *Electrochim. Acta* 40 (1995) 355.
- [8] M. Watanabe, H. Igarashi, K. Yosioka, *Electrochim. Acta* 40 (1995) 329.
- [9] J. Maruyama, M. Inaba, K. Katakura, Z. Ogumi, Z. Takehara, *J. Electroanal. Chem.* 447 (1998) 201.
- [10] E. Passalacqua, F. Lufrano, G. Squadrito, A. Patti, L. Giorgi, *Electrochim. Acta* 46 (2001) 799.
- [11] G. Sasikumar, J.W. Ihm, H. Ryu, *J. Power Sources* 132 (2004) 11.
- [12] U.A. Paulus, Z. Veziridis, B. Schnyder, M. Kuhnke, G.G. Scherer, A. Wokaun, *J. Electroanal. Chem.* 541 (2003) 77.
- [13] S.L.J. Gojkovic, S.K. Zecevic, R.F. Savinell, *J. Electrochem. Soc.* 145 (1998) 3713.
- [14] W.H. Lizcano-Valbuena, D.C.D. Azevedo, E.R. Gonzalez, *Electrochim. Acta* 49 (2004) 1289.
- [15] T.J. Schmidt, H.A. Gasteiger, G.D. Stab, P.M. Urban, D.M. Kolb, R.J. Behm, *J. Electrochem. Soc.* 145 (1998) 2354.
- [16] L.A. Zook, J. Leddy, *Anal. Chem.* 68 (1996) 3793.
- [17] F.C. Nart, W. Vielstich, Normalization of porous active surfaces, in: W. Vielstich, H.A. Gasteiger, A. Lamm (Eds.), *Handbook of Fuel Cells—Fundamentals, Technology and Applications*, vol. 2, John Wiley & Sons, 2003, pp. 301–315.
- [18] R.B. Lin, S.M. Shih, *J. Solid State Electrochem.* 10 (2006) 243.
- [19] R.B. Lin, S.M. Shih, *J. Chin. Inst. Chem. Eng.* 39 (2008) 475.
- [20] W.J. Liu, B.L. Wu, C.S. Cha, *J. Electroanal. Chem.* 476 (1999) 101.
- [21] K.H. Kangasniemi, D.A. Condit, T.D. Jarvi, *J. Electrochem. Soc.* 151 (2004) E125.
- [22] A.J. Bard, L.R. Faulkner, *Electrochemical Methods—Fundamentals and Applications*, Wiley, New York, 2001.
- [23] H.A. Gasteiger, N.M. Markovic, P.N. Ross, *J. Phys. Chem.* 99 (1995) 8290.
- [24] R.M.Q. Mello, E.A. Ticianelli, *Electrochim. Acta* 42 (1997) 1031.
- [25] H.S. Fogler, *Elements of Chemical Reaction Engineering*, Prentice-Hall, New Jersey, 1999.
- [26] G.F. Froment, K.B. Bischoff, *Chemical Reactor Analysis and Design*, John Wiley & Sons, New York, 1990.
- [27] J. Szekeley, J.W. Evans, H.Y. Sohn, *Gas–Solid Reaction*, Academic Press, London, 1976.
- [28] R.B. Lin, *Kinetics of Hydrogen Oxidation Reaction on Pt Catalysts Used in Fuel Cells*, PhD Dissertation, National Taiwan University, Taiwan, 2005.
- [29] J.H. Jiang, A. Kucernak, *J. Electroanal. Chem.* 567 (2004) 123.
- [30] N.M. Markovic, B.N. Grgur, P.N. Ross, *J. Phys. Chem.* 101 (1997) 5405.